# Antitumor Agents. 5. Synthesis, Structure−Activity Relationships, and Biological Evaluation of Dimethyl-5*H*-pyridophenoxazin-5-ones, Tetrahydro-5*H*-benzopyridophenoxazin-5-ones, and 5*H*-Benzopyridophenoxazin-5-ones with Potent Antiproliferative Activity

Adele Bolognese,*[,†,||] Gaetano Correale,[†] Michele Manfra,[†] Antonio Lavecchia,*[,‡,||] Ettore Novellino,[‡] and Stefano Pepe[§]

*Dipartimento di Chimica Organica e Biochimica, Università di Napoli "Federico II", Via Cynthia 6, Monte Sant'Angelo, I-80126 Napoli, Italy, Dipartimento di Chimica Farmaceutica e Tossicologica, Università di Napoli "Federico II", Via D. Montesano 49, I-80131 Napoli, Italy, and Dipartimento di Endocrinologia ed Oncologia Molecolare e Clinica, Università di Napoli "Federico II", Via S. Pansini 5, I-80131 Napoli, Italy*

*Received July 29, 2005*

New antiproliferative compounds, dimethyl-5*H*-pyrido[3,2-*a*]phenoxazin-5-ones (**1**−**6**), tetrahydro-5*H*-benzopyrido[2,3-*j*]phenoxazin-5-ones (**7**−**9**), and 5*H*-benzopyrido[3,2-*a*]phenoxazin-5-ones (**10**−**12**) were synthesized and evaluated against representative human neoplastic cell lines. Dimethyl derivatives **1**−**6** were more active against carcinoma than leukemia cell lines. The tetrahydrobenzo derivatives **7**−**9** were scarcely active, whereas the corresponding benzo derivatives **10**−**12** showed notable cytotoxicity against a majority of the tested cell lines. Molecular modeling studies indicated that the high potency of **10** and **11**, the most cytotoxic compounds of the whole series, could be due to the position of the condensed benzene ring, which favors $\pi-\pi$ stacking interactions with purine and pyrimidine bases in the DNA active site. Biological studies suggested that **10**−**12** have no effect on human topoisomerases I and II and that they induce arrest at the G2/M phase.

## Introduction

Anticancer quinones are currently the focus of intensive research because of their biological activity and their intricate modes of action. Anthracyclines, actinomycin D, streptonigrin, and mitomycin C, produced by different strains of streptomyces, and synthetic epirubicin and mitoxantron are well-known examples of quinones acting as antiproliferative drugs.[1−4] Although these and other quinonoid compounds are effective in the treatment of many different forms of cancer, their side effects (the most severe being cumulative heart toxicity) limit their use.[5,6] The antineoplastic activity of these drugs is the result of strong interaction with DNA in the target cells, which causes degradation of the nucleic acid structure and, consequently, terminates its biological function.[7] The planar system of these drugs can intercalate between the DNA base pairs, where major contributions to binding arise from hydrogen bonding and/or electrostatic, van der Waals, and hydrophobic interactions. At the same time, the quinone moiety of these agents can also undergo enzymatic reduction. In the presence of molecular oxygen, the resulting semiquinone and hydroquinone produce reactive oxygen species or ROS[8] (superoxide radical anions, hydrogen peroxide, and hydroxyl radicals) in a process known as redox cycling. ROS are detrimental to cellular macromolecules in that they are capable of causing DNA strand scission, protein oxidation, and other lesions. The production of semiquinones and/or hydroquinones by enzymatic reduction is strongly dependent on the presence of electron-withdrawing or electron-donating groups on the quinone system.

In a recent article,[9] we described the synthesis and biological activity of 5*H*-pyrido[3,2-*a*]phenoxazin-5-one (PPH, Chart 1), a new anticancer iminoquinone, and a series of its derivatives that are able to inhibit a large number of lymphoblastoid and solid tumor-derived cells at submicromolar concentrations. Molecular modeling studies and NMR investigations suggested that the cytotoxic activity of PPH results from the intercalation at the middle 5′-GC-3′ base pairs of DNA,[9] involving the formation of two strong hydrogen bonds between the hydrogen of the positively charged pyridine nitrogen of PPH and both the O4′ atom in the deoxyribose ring of the cytosine C5 residue and the O5′ atom of the phosphate backbone located between the G4 and C5 residues of a $[d(GAAGCTTC)]_2$ octamer. Additional stability of the complex arises from $\pi-\pi$ stacking interactions between the tetracyclic pyridophenoxazinone system and the aromatic base rings.

In a further study,[10] we considered the influence of single substituents on ring A of PPH and showed that electron-withdrawing groups increase antiproliferative potency, whereas electron-donating groups slightly decrease cytotoxicity. Nevertheless, five cancer cell lines, three lymphoma/leukemia cells (Wil2-NS, MT-4 and CCRF-SB) and two carcinoma (ACHN and 5637) cells, were very sensitive to the antiproliferative effect of some monomethyl derivatives, suggesting that the substituents may play different roles in cytotoxic potency as well as in specificity. Therefore, to evaluate the influence of lipophilicity, steric hindrance, and chromophore extension on antiproliferative activity, we designed and synthesized a series of disubstituted derivatives of PPH (Chart 1), holding two methyl groups at all free positions of ring A (compounds **1**−**6**), a cyclohexenyl ring (compounds **7**−**9**), and a benzo ring (compounds **10**−**12**) condensed at the 10,11-, 9,10-, and 8,9-double bond, respectively, of ring A.

## Results and Discussion

**Chemistry**. Condensation of substituted 2-aminophenols and quinolin-5,8-dione (**QQ**), in acetic acid, yielded dimethyl-5*H*-pyrido[3,2-*a*]phenoxazin-5-ones (**1**−**6**), tetrahydro-5H-benzopyridophenoxazin-5-ones (**7**−**9**), and 5*H*-benzopyridophenoxazin-

* To whom correspondence should be addressed. Tel: +39-081-674121. Fax: +39-081-674393. E-mail: bologne@unina.it (A.B.). Tel: +39-081-678613. Fax: +39-081-678613. E-mail: lavecchi@unina.it (A.L.).
† Dipartimento di Chimica Organica e Biochimica.
‡ Dipartimento di Chimica Farmaceutica e Tossicologica.
§ Dipartimento di Endocrinologia ed Oncologia Molecolare e Clinica.
|| These authors contributed equally to this work.

10.1021/jm050745l CCC: $33.50 © 2006 American Chemical Society
Published on Web 07/28/2006

**Chart 1**

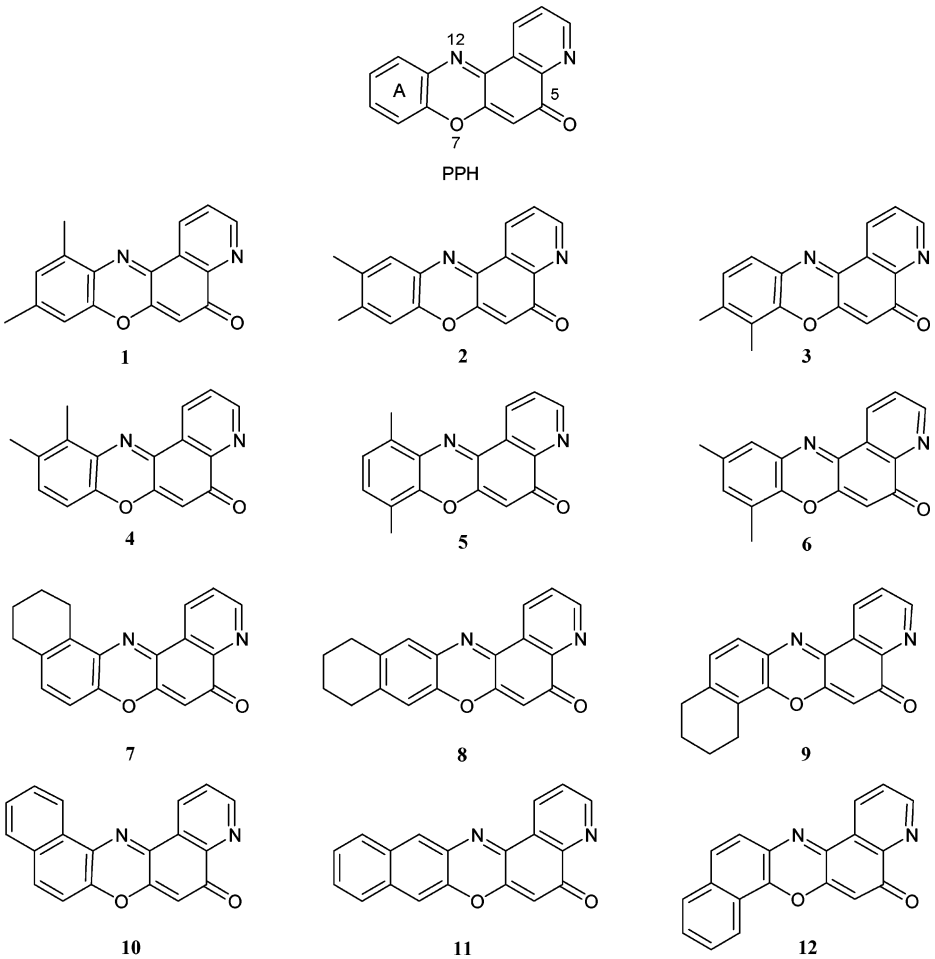


**Scheme 1**

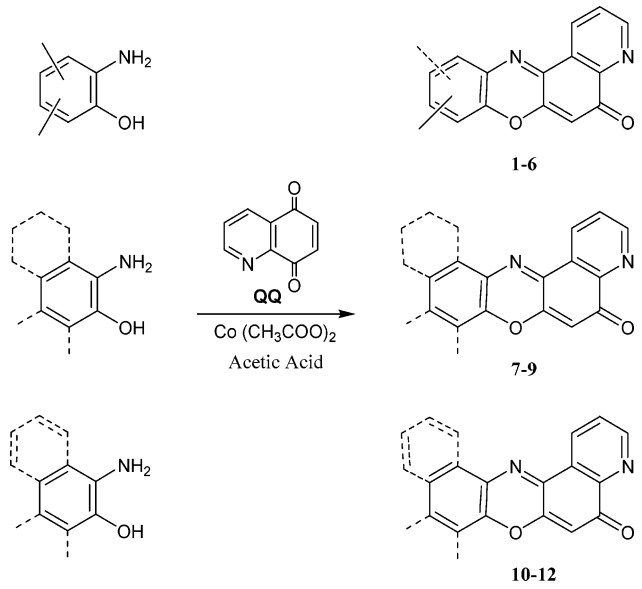


5-ones (**10**−**12**) (Scheme 1). The products were obtained in moderate yields because of the formation of intractable black materials due to the oxidation of *o*-aminophenols.

To synthesize compounds **1**−**9**, suitable 3, 5-, 4,5-, 5,6-, 3,4-, 3,6- and 4,6-dimethyl 2-aminophenols were employed for **1**−**6** and 1-amino-5,6,7,8-tetrahydronaphthalen-2-ol, 3-amino-5,6,7,8-tetrahydro- and 2-amino-5,6,7,8-tetrahydronaphthalen-1-ol for **7**−**9**. To prepare the benzofused **10**−**12**, the corresponding 1-amino-, 3-amino-naphthalen-2-ol, and 2-amino-naphthalen-1-ol were also used. To enhance the yield of compounds, the reactions were performed according to a previously reported procedure,[9] using Co(II) acetate. The formation of the Co(II)/quinolin-5,6-dione complex, which promotes a charge density at the 6 position of **QQ**, pushes the reaction to form the 5*H*-pyridophenoxazinones of interest to us. Scheme 2 depicts the mechanism of formation of compounds **1**−**12** via a multistep reaction involving two molecules of 2-aminophenol named X and Y, respectively. The reaction starts with a 1,4-Michael addition of the amino group of X at the 6 position of the α,*β*-unsatured system of quinolin-5,8-dione complexed with the cobalt ion. Quinone reduction takes place, and it is followed by reoxidation by oxygen or by the quinone present in situ. Subsequently, an intramolecular attack of the hydroxyl group of X to the carbonyl carbon in the 5 position gives rise to a hemiketal, which undergoes a substitution reaction by the amino group of Y, yielding the corresponding iminoquinone compound. The latter drives away the *o*-aminophenol X, yielding the 5*H*-pyrido[3,2-*a*]phenoxazin-5-ones (**1**−**12**), after rearrangement and oxidation. Under these conditions, the formation of the 5*H*-pyrido[2,3-*a*]phenoxazin-5-one isomer is disfavored because a low charge density is present at the 7 position.

All of the compounds were characterized on the basis of their chemical and spectroscopic properties and by elemental analysis. The structural assignments were also accomplished through extensive 2D NMR spectroscopy, HMQC, and HMBC. In the HMBC spectra of **10**, selected as a representative compound, the double-doublet assigned to the more deshielded H3 proton at $\delta_H$ 9.15 shows a very significant strong correlation with the

**Scheme 2**

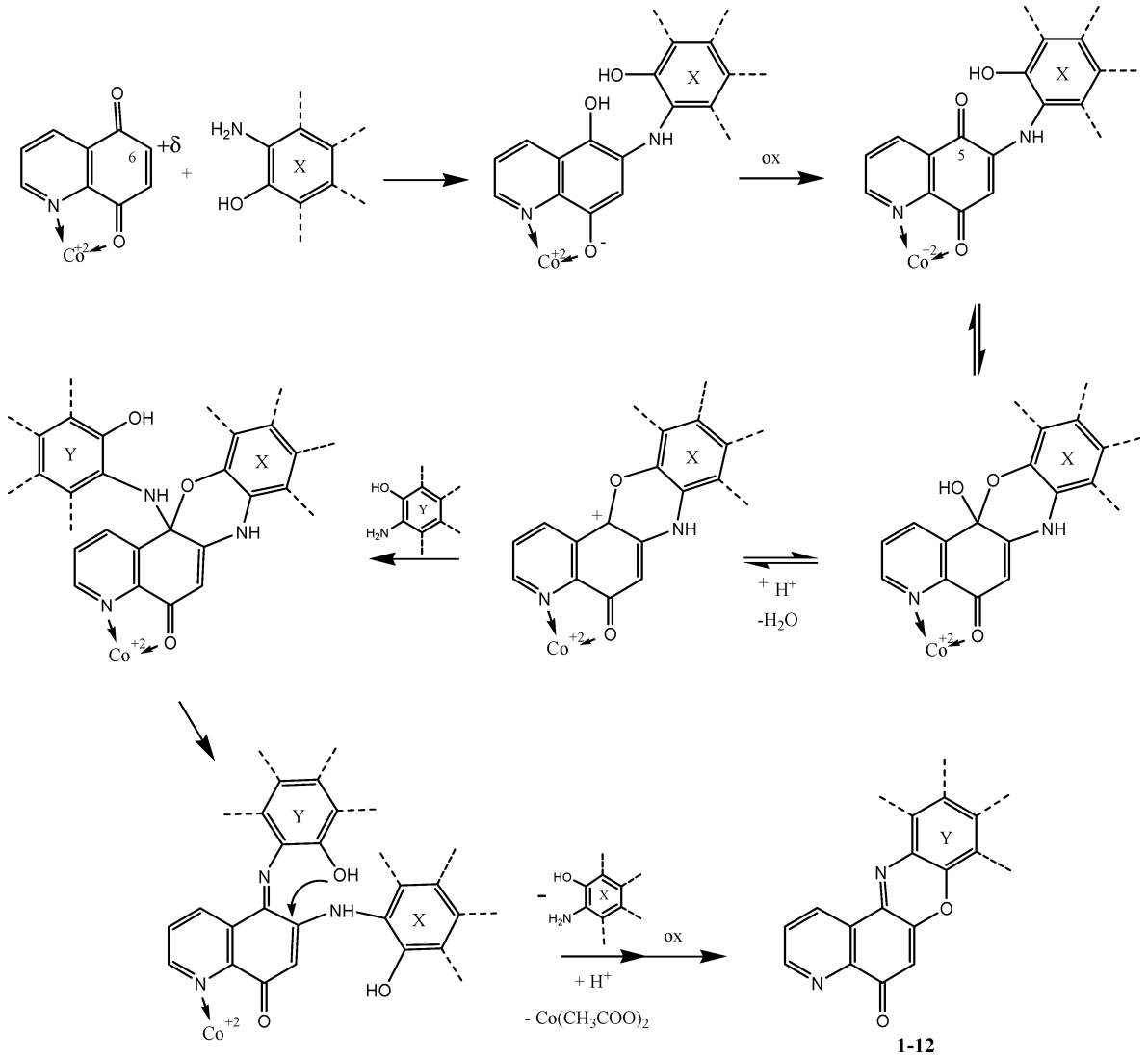


signals at $\delta_C$ 155.10 (C4a) and 134.8 (C1). The proton H1 at $\delta_H$ 8.71 correlates with the signals at $\delta_C$ 153.60 (C3) and 155.10 (C4a), whereas the double-doublet at $\delta_H$ 7.70, assigned to the H2 proton correlates with the signal at $\delta_C$ 135.83 (C14b). The quinonic proton H6, lying at $\delta_H$ 6.69, correlates with the signal at $\delta_C$ 155.10 (C4a). This relation unambiguously validates the attributions of signals that are typical of the quinolinquinonic moiety of compounds **1**−**12**. Figure 1 depicts HMBC relations in **10**.

**Antiproliferative Activity.** The antiproliferative activity of the PPH alkyl derivatives **1**−**9** was evaluated against a panel of 13 human cell lines representative of liquid and solid human tumors, and the results are shown in Tables 1 and 2. Data for the anticancer agents PPH, doxorubicin, and AMD are included for comparison.

Initial SAR studies were focused on the effects of the dimethyl substitution on benzo-fused ring A of PPH. Compounds **1** and **2**, with two methyl groups at the 9,11- and 9,-10-positions of ring A, were the most cytotoxic compounds with median values of 0.1 $\mu$M (range 0.001−0.5 $\mu$M) and 0.3 $\mu$M (range 0.03−0.9 $\mu$M), respectively. Dimethyl derivatives **3**, **5**, and **6** were less active than **1** and **2**, with a median $IC_{50}$ value ranging between 0.5 and 0.9 $\mu$M, and they were also 50-, 70-, and 90-fold less active than PPH. Compound **4**, which has two methyl groups at the 10,11-positions, was found to be 120-fold less active than PPH (median $IC_{50}$ = 1.2 $\mu$M, range 0.2−2.7 $\mu$M). The $IC_{50}$ values obtained for dimethyl derivatives **1**−**6** clearly show that the position of substituents on phenyl ring A greatly affects cytotoxic activity. The compound methylated on the 10,11-positions (**4**) showed low activity, whereas compounds methylated on the 8,11- and 8,10-positions (**5** and **6**) were only moderately active. In contrast, substitution at the 9,10-positions (**2**) was tolerated and substitution at the 9,11-positions (**1**) was optimal. Moreover, the dimethyl derivatives **1** and **2** displayed an enhanced specificity toward some tumor cell lines compared with the corresponding monomethylated analogues previously described.[10] Compound **2** revealed a distinct specificity toward two lymphoma/leukemia cells, $CD4^+$ acute T-lymphoblastic leukemia (C8166) and acute B-lymphoblastic leukemia (CCRF-SB) as well as two carcinoma cells, colon adenocarcinoma (HT-29) and nasopharyngeal carcinoma (KB). Compound **5** exhibited specificity against 5637 carcinoma cells and MT-4 leukemia cells. Finally, compound **6** displayed this behavior against ACHN carcinoma cells. Taken together, these results suggest that dimethyl derivatives **1**−**3** and **5** display better specificity as antiproliferative agents against the carcinoma cell lines than against the leukemia cell lines. Moreover, a comparison between the antiproliferative activities of the previously reported monomethyls[10] and the dimethyl derivatives presented here still suggests that some carcinoma cell lines, such as G361, ACHN, 5637,

**Table 1.** Antitumor Activity of **1**−**12** and PPH against Leukemia/Lymphoma Cells

| | $IC_{50}$ ($\mu$M)[a] | | | | | |
|---|---|---|---|---|---|---|
| | leukemia/lymphoma | | | | | |
| compd | Wil2-NS | MOLT-4 | C8166 | MT-4 | CCRF-SB | CCRF-CEM |
| **1** | 0.07 ± 0.003 | 0.5 ± 0.02 | 0.2 ± 0.03 | 0.04 ± 0.001 | 0.02 ± 0.002 | 0.1 ± 0.02 |
| **2** | 0.4 ± 0.02 | 0.3 ± 0.01 | 0.04 ± 0.04 | 0.1 ± 0.02 | 0.04 ± 0.004 | 0.15 ± 0.02 |
| **3** | 1.8 ± 0.2 | 3.0 ± 0.2 | 0.5 ± 0.01 | 0.3 ± 0.01 | 0.1 ± 0.02 | 6.0 ± 0.2 |
| **4** | 2.0 ± 0.2 | 2.7 ± 0.1 | 1.1 ± 0.1 | 0.3 ± 0.2 | 1.2 ± 0.3 | 0.2 ± 0.01 |
| **5** | 1.1 ± 0.1 | 1.6 ± 0.2 | 8.0 ± 0.3 | 0.08 ± 0.003 | 0.4 ± 0.02 | 0.7 ± 0.03 |
| **6** | 0.9 ± 0.02 | 1.2 ± 0.2 | 0.5 ± 0.03 | 0.1 ± 0.01 | 0.3 ± 0.03 | 0.15 ± 0.02 |
| **7** | 4.0 ± 0.3 | 3.2 ± 0.2 | 2.0 ± 0.1 | 1.3 ± 0.1 | 1.0 ± 0.1 | 1.3 ± 0.02 |
| **8** | 1.2 ± 0.2 | 1.8 ± 0.1 | 1.0 ± 0.1 | 1.5 ± 0.2 | 2.0 ± 0.2 | 1.1 ± 0.1 |
| **9** | 2.1 ± 0.3 | 1.9 ± 0.1 | 1.0 ± 0.1 | 1.5 ± 0.1 | 1.4 ± 0.1 | 1.9 ± 0.2 |
| **10** | 0.005 ± 0.0004 | 0.04 ± 0.002 | 0.001 ± 0.0001 | 0.01 ± 0.002 | 0.01 ± 0.001 | 0.001 ± 0.0002 |
| **11** | 0.01 ± 0.001 | 0.01 ± 0.003 | 0.02 ± 0.001 | 0.05 ± 0.002 | 0.01 ± 0.002 | 0.004 ± 0.0003 |
| **12** | 0.06 ± 0.004 | 0.09 ± 0.001 | 0.1 ± 0.002 | 0.1 ± 0.03 | 0.02 ± 0.004 | 0.05 ± 0.002 |
| PPH | 0.05 | 0.04 | 0.10 | 0.02 | 0.01 | 0.01 |
| doxo[b] | 0.02 | 0.02 | 0.02 | 0.01 | 0.02 | 0.03 |
| AMD[b] | 0.003 | 0.001 | 0.0008 | 0.0009 | 0.002 | 0.001 |

[a] The compound concentration required to reduce cell proliferation by 50%, as determined the MTT method, under conditions allowing untreated controls to undergo at least three consecutive rounds of multiplication. Data represent $IC_{50}$ mean values for three independent determinations ± standard error of the $IC_{50}$ mean. Wil2-NS, human splenic B-lymphoblastoid cells; MOLT-4, human acute T-lymphoblastic leukemia; C8166 and MT-4, $CD4^+$ human acute T-lymphoblastic leukemia; CCRF-SB, human acute B-lymphoblastic leukemia; CCRF-CEM, human acute T-lymphoblastic leukemia. [b] The doxo and AMD compounds were used as controls.

**Table 2.** Antitumor Activity of **1**−**12** and PPH against Carcinoma Cells

| | $IC_{50}$ ($\mu$M)[a] | | | | | | |
|---|---|---|---|---|---|---|---|
| | carcinoma | | | | | | |
| compd | G361 | HT-29 | HeLa | Hep-2 | ACHN | 5637 | KB |
| **1** | 0.001 ± 0.0001 | 0.2 ± 0.03 | 0.2 ± 0.04 | 0.3 ± 0.03 | 0.001 ± 0.0004 | 0.005 ± 0.0005 | 0.3 ± 0.04 |
| **2** | 0.9 ± 0.04 | 0.03 ± 0.001 | 0.8 ± 0.02 | 0.8 ± 0.03 | 0.4 ± 0.03 | 0.8 ± 0.04 | 0.09 ± 0.01 |
| **3** | 0.03 ± 0.003 | 6.9 ± 0.1 | 0.6 ± 0.03 | 0.4 ± 0.02 | 0.005 ± 0.003 | 1.8 ± 0.2 | 0.4 ± 0.03 |
| **4** | 1.3 ± 0.2 | 1.2 ± 0.3 | 2.6 ± 0.4 | 1.3 ± 0.2 | 1.8 ± 0.1 | 0.9 ± 0.01 | 0.7 ± 0.02 |
| **5** | 0.7 ± 0.02 | 5.5 ± 0.04 | 0.9 ± 0.02 | 0.4 ± 0.03 | 0.5 ± 0.02 | 0.01 ± 0.004 | 0.5 ± 0.01 |
| **6** | 1.5 ± 0.2 | 1.6 ± 0.2 | 1.7 ± 0.1 | 1.1 ± 0.1 | 0.9 ± 0.02 | 0.6 ± 0.1 | 1.2 ± 0.1 |
| **7** | 1.3 ± 0.1 | 1.0 ± 0.2 | 1.6 ± 0.2 | 1.9 ± 0.2 | 1.8 ± 0.1 | 1.9 ± 0.1 | 1.7 ± 0.1 |
| **8** | 1.5 ± 0.3 | 3.3 ± 0.2 | 1.1 ± 0.1 | 1.7 ± 0.1 | 1.4 ± 0.1 | 1.0 ± 0.1 | 1.0 ± 0.2 |
| **9** | 2.0 ± 0.1 | 2.1 ± 0.1 | 2.5 ± 0.2 | 1.8 ± 0.2 | 1.9 ± 0.2 | 1.1 ± 0.1 | 1.0 ± 0.1 |
| **10** | 0.02 ± 0.002 | 0.002 ± 0.0003 | 0.001 ± 0.0004 | 0.04 ± 0.004 | 0.01 ± 0.003 | 0.01 ± 0.001 | 0.01 ± 0.003 |
| **11** | 0.01 ± 0.004 | 0.03 ± 0.004 | 0.05 ± 0.01 | 0.05 ± 0.002 | 0.02 ± 0.003 | 0.02 ± 0.002 | 0.02 ± 0.002 |
| **12** | 0.05 ± 0.005 | 0.3 ± 0.03 | 0.2 ± 0.01 | 0.06 ± 0.003 | 0.5 ± 0.04 | 0.1 ± 0.02 | 0.1 ± 0.02 |
| PPH | 0.01 | 0.20 | 0.20 | 0.04 | 0.01 | 0.01 | 0.1 |
| doxo[b] | 0.09 | 0.15 | 0.07 | 0.04 | 0.04 | 0.02 | 0.15 |
| AMD[b] | 0.001 | 0.006 | 0.04 | 0.004 | 0.005 | 0.003 | 0.001 |

[a] The compound concentration required to reduce cell proliferation by 50%, as determined the MTT method, under conditions allowing untreated controls to undergo at least three consecutive rounds of multiplication. Data represent $IC_{50}$ mean values for three independent determinations ± standard error of the $IC_{50}$ mean. G361, human skin melanoma; HT-29, human colon adenocarcinoma; HeLa, cervix carcinoma; Hep-2, larynx carcinoma; ACHN, human renal adenocarcinoma; 5637, human bladder carcinoma; KB, human nasopharyngeal carcinoma. [b] The doxo and AMD compounds were used as controls.

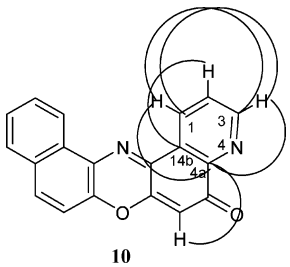


**10**

**Figure 1.** Most significant structural relations in the quinolinquinonic moiety of **10** by HMBC.

HT-29, seem to be more sensitive to the dimethyl derivatives than to monomethyl derivatives with the methyl group at the same position of one of two methyls. In particular, **1**, **2**, and **3**, when compared with the 9-monomethyl derivative, showed higher activity against some cell lines (G361, ACHN, 5637, and HT-29 for **1**; HT-29, C8166, and ACHN for **2**; and CCRF-CEM, G361, and ACHN for **3**). Also for **1** and **5**, some carcinoma cell lines were more sensitive (G361, HT-29 for **1** and 5637 for **5**). Among **2**, **4**, and **5**, only **2** was more active than the 10-monomethyl against C8166 and HT-29. Finally, among **3**, **5**, and **6**, compounds **3** and **5** were more active than 8-monomethyl against some cell lines (G361, ACHN for **3**) and (5637 for **5**).

The good antiproliferative activity and the specificity against carcinoma cells showed by dimethyl derivatives could imply that lipophilic and bulky substituents at ring A increase cytotoxic potency. To test this hypothesis, we synthesized and evaluated for cytotoxic activity the more lipophilic and hindered pentacyclic derivatives **7**−**9** (Chart 1), characterized by having a cyclohexenyl ring condensed at the 10,11-, 9,10-, and 8,9-positions of ring A, respectively. The data collected in Tables 1 and 2 show that these compounds have an antiproliferative activity significantly lower than that exerted by the corresponding dimethyl derivatives **4**, **2**, and **3** in all of the examined cell lines. In particular, **7**, **8**, and **9** exhibited a median $IC_{50}$ value ranging between 1.4 and 1.9 $\mu$M and were equipotent to **4**. On the contrary, **2** and **3** were 1 order of magnitude more potent than the corresponding cyclohexyl derivatives **8** and **9**. This comparison suggests that the increasing of lipophilicity and steric

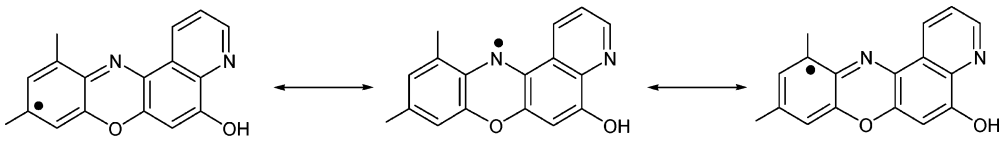

**1**

**Figure 2.** Resonance structures of the radical of compound **1**.

hindrance is detrimental when the cyclohexyl occupies both the 6,7- and 8,9-positions, and does not affect the antiproliferative activity when it is at 10,11-positions.

As regards the dimethyl derivatives, the high cytotoxicity of **1**−**3** could be due to oxidative DNA damage via a conversion of oxygen into DNA-cleaving oxygen radicals. Numerous studies on quinone and iminoquinone compounds indicated that there is a quantitative linear relationship between their reduction potentials and the rate at which they degrade DNA in vitro.[11,12]

In a previous article, we reported that the pyridophenoxazinone system of PPH undergoes enzymatic single-electron reduction to a free radical intermediate by reducing agents present in the biological system. The transfer of the unpaired electron to the oxygen yields the superoxide, which can cause intracellular macromolecular damage and cell death. This could account for the cytotoxic activity of pyridophenoxazinones **1**−**6**, which possess an iminoquinone function capable of involving a one electron redox reaction. Of note is the fact that in a quinonoid system, the redox potential and the stability of the corresponding radical are both related to the presence of substituent groups. Regarding the formation and stability of the phenoxy radical, it was reported that the effect of a substituent changes with the change in substituent position and that electron-donating groups at the para position stabilize the radical.[14] In light of these arguments, the high cytotoxic activity exhibited by **1**−**3** holding electron-donating methyl groups in para position to the heterocycle nitrogen, could be ascribed to an extra stability of the corresponding radicals. Figure 2 shows the resonance structures of the radical of compound **1**, which could contribute to its stability.

As stated previously,[9] in the intercalation model of PPH, ring A plays a crucial role in the stabilization of the PPH/DNA complex through $\pi-\pi$ stacking interactions. Therefore, to improve DNA intercalation, we extended the aromatic system of PPH in all three directions of annulation by condensation of a benzene at the 10,11-, 9,10-, and 8,9-double bond of ring A (**10**−**12**). The cytotoxicity of each of these compounds was evaluated and is shown in Tables 1 and 2. In general, compounds **10** and **11** exhibited the highest cytotoxic potency across the panel of lymphoblastoid and carcinoma cell lines, with a median $IC_{50}$ value of 0.01 and 0.02 $\mu$M, respectively. A significant inhibitory effect of **10** was observed on the proliferation of the limphobastoid cell lines, with the lowest $IC_{50}$ values for Wil2-NS ($IC_{50}$ = 0.005 $\mu$M), C8166 and CCRF-CEM ($IC_{50}$ = 0.001 $\mu$M). Carcinoma cells HT-29 and HeLa were also very sensitive ($IC_{50}$ = 0.002 and 0.001 $\mu$M, respectively). Among the tumor cell lines, the CCRF-CEM cells were the most prone to the antiproliferative effect of **11** ($IC_{50}$ = 0.004 $\mu$M). Compound **12**, holding the benzo-fused ring at 8,9 positions, resulted in a notable decrease in potency with respect to that of **10** and **11** and was almost equipotent to PPH.

**DNA Binding Studies.** A typical UV−visible titration experiment was carried out to investigate the DNA-binding behavior of **1**, **2**, **7**, **8**, and **10**, representative members of each group of the pyridophenoxazinone derivatives. Their spectroscopic properties, in the presence and absence of calf thymus DNA, were studied by conventional optical spectroscopy. Compounds **7** and **8** did not exhibit hypochromic or bathochromic effects on its UV spectrum in the presence of DNA, thus confirming the very weak interaction of these compound with DNA. Compounds **1** and **2** exhibited a bathochromic shift of 6 nm (from 454 to 460 nm and from 459 to 465 nm, respectively) and a corresponding reduction in extinction coefficient of about 11% and 20% on binding, whereas compound **10** showed a wavelength shift of 16 nm (from 477 to 493 nm) accompanied by a hypochromicity of about 20%. Such perturbations, which are characteristic of the stacking interactions involved in the intercalation process, seem to be in accordance with the above-mentioned cytotoxic trend. The presence of one isosbestic point for **1** (581 nm) and two isosbestic points for both **2** (298 and 572 nm) and **10** (315 and 454 nm) indicates the existence of a single binding mode with DNA.

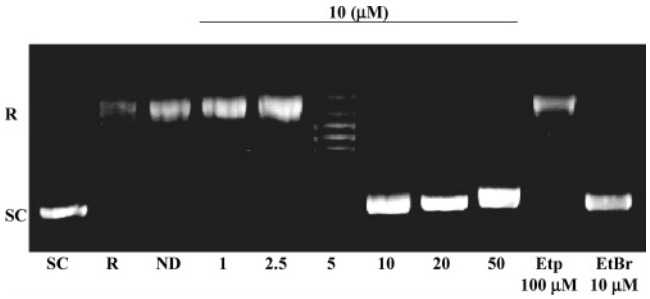


**Figure 3.** Agarose gel stained with ethidium bromide. Compound **10** intercalates into DNA. Intercalation was monitored by conversion of relaxed plasmid DNA to supercoiled molecules. Control reactions were carried out in the absence of topoisomerase I or the drug (SC = Supercoiled; R = Relaxed; ND = No Drug; Etp = Etoposide; EtBr = Ethidium Bromide). A titration of **10** (1−50 $\mu$M) was carried out with constant topoisomerase I concentration. Reactions containing Etp (100 $\mu$M) and EtBr (10 $\mu$M) are included as examples of a nonintercalative and intercalative drug, respectively.

To establish the intercalative nature of this series of compounds, a DNA unwinding assay was performed on the most active **10**. Because intercalative drugs locally unwind DNA, they induce compensatory unconstrained positive superhelical twists in distal regions of covalently closed circular DNA.[15] Therefore, in the presence of an intercalative compound, a plasmid that is relaxed (i.e., contains no superhelical twists) becomes positively supercoiled. The treatment of drug−DNA complexes with mammalian topoisomerase I removes the unconstrained positive DNA superhelical twists that result from drug intercalation.[16] Following this treatment, extraction of the compound allows the constrained local drug-induced unwinding to redistribute in a global manner and manifest itself as a net negative supercoiling of the plasmid. Thus, in the presence of an intercalative agent such as ethidium bromide, topoisomerase I treatment converts relaxed plasmids to negatively supercoiled molecules. Conversely, when a nonintercalative drug such as etoposide is included in reaction mixtures, no DNA supercoiling is observed following treatment with the type I enzyme.

As seen in Figure 3, relaxed plasmid substrates were converted to negatively supercoiled molecules by treatment with topoisomerase I in the presence of 1−50 $\mu$M of compound **10**.

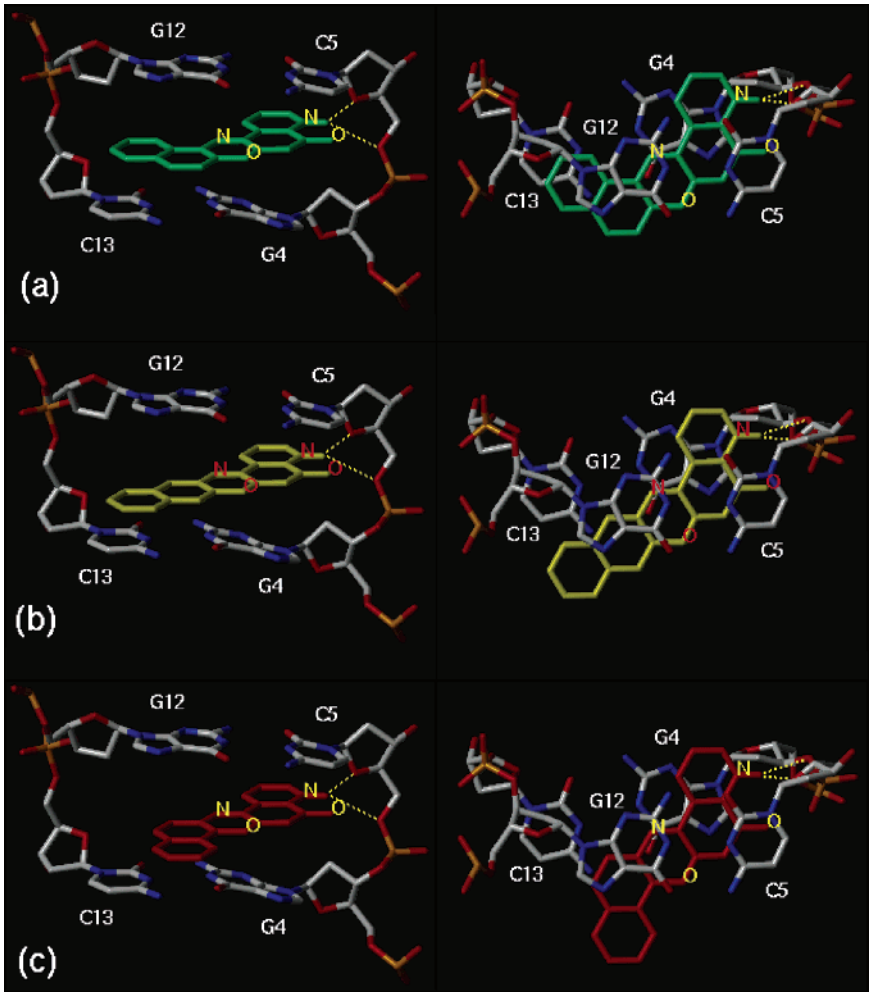


**Figure 4.** Intercalation site of the **10**/[d(GAAGCTTC)]$_2$ (a), **11**/[d(GAAGCTTC)]$_2$ (b), and **12**/[d(GAAGCTTC)]$_2$ (c) complexes viewed in a projection plane parallel (on the left) and orthogonal (on the right) to the helix axis.

The midpoint of the transition was approximately 5 $\mu$M of the drug and complete unwinding was observed at approximately 20 $\mu$M. Taken together, these findings provide strong evidence that **10** binds to DNA in an intercalative manner, suggesting an analogous behavior for the whole series. On the basis of these evidences, if one assumes that compound **10** occupies the same position of PPH in the DNA intercalation site, the difference in potency observed for **10**−**12** could be ascribed to their different abilities to form $\pi-\pi$ stacking interactions with purine and pyrimidine bases in the DNA active site (GC−CG of opposite strands). To analyze this aspect, we undertook a molecular modeling study. Insight into the mode of binding of **10**−**12** to DNA was gained through molecular mechanics using the DNA octamer [d(GAAGCTTC)]$_2$. The sequence was selected according to the experimental binding preferences demonstrated by some phenoxazinones.[9,17]

The complexes were constructed by overlapping the structures of **10**−**12** to that of PPH in the previously published PPH/[d(GAAGCTTC)]$_2$ complex model.[9] The pyridine nitrogen of the ligands was taken as protonated, as suggested from the p*K*a of their conjugated acid. The structure of PPH was then removed, and the energy of the resulting complexes was minimized with SYBYL,[18] using the Tripos force field.[19] During energy minimization, the structure of the nucleic acid was frozen, while the ligands were allowed to move.

The DNA binding models of **10**, **11**, and **12** (Figure 4) display the presence of two strong hydrogen bonds between the hydrogen of the positively charged pyridine nitrogen and both the O4′ and O5′ atoms of the octamer phosphate backbone. However, **10** projects its naphthyl ring properly to form $\pi$-stacking interactions with guanine G12 and cytosine C13, whereas compound **11** projects the same group near guanine G12 but beyond cytosine C13. On the contrary, the naphthyl ring of compound **12** protrudes out of the DNA duplex, thus reducing the interaction. These results seem to suggest that the different cytotoxicities observed for **10**−**12** can be related to the different spatial orientation of the naphthyl ring with respect to the DNA base pairs.

To obtain more insight into the possible mechanism of action of compounds **10**−**12**, which manifested the most interesting antiproliferative activity, topoisomerase assays and cell cycle measurements were performed.

**Effects of 10**−**12 on the Cell Cycle.** Treatment of HT-29 human colon carcinoma cells with **10**−**12** for 24 h led to profound changes of the cell cycle profiles (Figure 5).

The flow cytometry analysis of propidiumiodide-labeled cells indicates that the cytotoxic drugs **10** and **11** induce a block in the G2/M phase, whereas **12** seems to provoke both a late S-phase accumulation and a G2/M block.The G2 cell population increases from 14.15% in the control to 48.66% for **10** and 55.01% for **11**, whereas the G0/G1 and S-phase cell populations gradually decrease from 47.74% and 38.11% to 27.93% and 23.42% for **10** and to 24.06% and 20.93% for **11**. For compound **12**, both G2 and S-phase cell populations increase to 38.49% and 43.88%, respectively, whereas the G0/G1 phase decreases to 17.63%. This latter occurrence may reflect an action of **12**

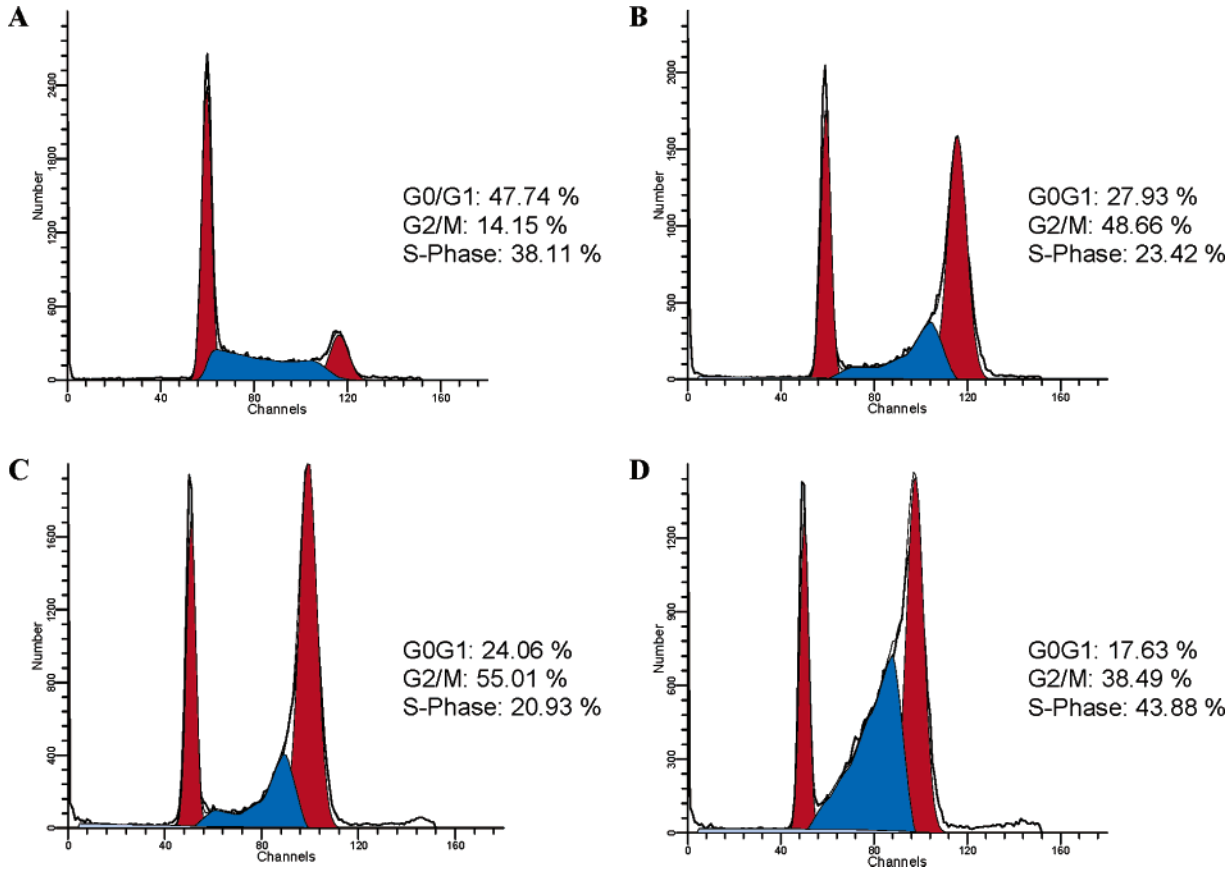


**Figure 5.** Effect of compounds **10**−**12** on the cell cycle of HT-29 cells. The cells were untreated (A) and treated with 1 mM concentration of **10** (B), **11** (C), and **12** (D) for 24 h, fixed, and stained with propidium iodide to determine the nuclear DNA content. The percentage of cells in each phase of the cell cycle was obtained by flow cytometric analysis.

on two different targets and/or the activation of two independent cell death pathways. The concentrations required to elicit these effects on cell cycle are in agreement with the corresponding $IC_{50}$ values measured in the previous cytotoxic assays.

Because the cell cycle arrest at the G2/M boundary may be associated with poisoning of topoisomerase activity,[20] we studied the effects of compounds **10**−**12** on human DNA topoisomerases using a conventional DNA relaxation assay.

**Effects of 10**−**12 on Topoisomerases.** Supercoiled DNA was treated with either topoisomerase I or topoisomerase II in the presence of the test drugs at 10 or 50 $\mu$M, and the DNA relaxation products were then resolved by agarose gel electrophoresis. The analyzed compounds were not able to promote DNA cleavage by topoisomerases (data not shown). The amount of nicked (for topoI) or linear (for topoII) DNA species remains very weak in the presence of the tested drugs, in contrast to what was observed with the reference drugs camptothecin and etoposide, which produce a high level of single or double strand breaks, respectively. Therefore, **10**−**12** cannot be considered as topoisomerase poisons.

In conclusion, this study reports the synthesis and the SARs of a series of dimethyl- (**1**−**6**), tetrahydrobenzo- (**7**−**9**), and benzopyridophenoxazin-5-ones (**10**−**12**), analogues of PPH, exhibiting activity against leukemia and solid tumor cell lines at micromolar and submicromolar concentrations. Among the dimethyl derivatives, **1** and **2** displayed high specificity toward some tumor cell lines compared with that of the corresponding monomethylated analogues previously described.[10] The benzopyridophenoxazinones **10** and **11**, characterized by an extended aromatic system, were found to exhibit enhanced $\pi-\pi$ stacking interactions with DNA bases, which explains the associated high cytotoxic activity. We also analyzed the effect of **10**−**12** on cell cycle progression by flow cytometric analysis. Compounds **10** and **11** arrested HT-29 human colon carcinoma cells at the G2/M phase, whereas **12** seemed to provoke both a late S-phase accumulation and a G2/M block. None of the analyzed compounds involved the poisoning of topoisomerases in their mode of action. Clearly, these results provide a challenge for future studies on the mechanisms that contribute to the cytotoxicity of the pyridophenoxazinones.

## Experimental Section

**Chemistry.** Melting points were determined by a Kofler apparatus and are uncorrected. The elemental analysis (C, H, and N) of reported compounds agrees with the calculated values and was within ±0.4% of theoretical values. Electron impact (EI) mass spectra were obtained at 70 eV on a ZAB 2F spectrometer. UV spectra were recorded on Varian Cary 5000 UV−Vis−NIR Spectrophotometer. The purity of compounds was checked by ascending chromatography on silica gel Merck TLC F254 plates (Art. no. 105715). NMR measurements (data reported in $\delta$) were performed on a Bruker AMX-500 spectrometer equipped with a Bruker X-32 computer, using the UXNMR software package. NMR spectra were measured at 500 MHz ($^1$H) and 125 MHz ($^{13}$C). The chemical shifts are referenced to $^{13}CDCl_3$ and $CDCl_3$ solvent signals at 77.0 and 7.26 ppm, respectively. Standard pulse sequences were employed for magnitude COSY. HMQC and HMBC experiments were optimized for $^1J_{C-H}$ = 135 Hz and $^{2,3}J_{C-H}$ = 10 Hz, respectively. $Me_4Si$ was used as the internal reference. All reagents used in syntheses were commercial products: 2-amino-4,6-dimethylphenol (TLC Europe N. V., Belgium), 6-amino-2,3-dimethylphenol (Aurora Fine Chemicals, Austria), 3-amino-5,6,7,8-tetrahydronaphthalen-2-ol (Aldrich, U.S.A.), 2-aminonaphthalen-1-ol (ABCR GmbH & Co. KG, Germany), 3-aminonaphthalen-2-ol (ABCR

GmbH & Co. KG, Germany), 1-aminonaphthalen-2-ol (ABCR GmbH & Co. KG, Germany), 3,5-dimethyl-2-nitrophenol (Aldrich, USA), 3,4-dimethyl-2-nitrophenol (TLC Europe N. V., Belgium), 3,6-dimethyl-2-nitrophenol (Aurora Fine Chemicals, Austria), 4,5-dimethyl-2-nitrophenol (Aurora Fine Chemicals, Austria), 5,6,7,8-tetrahydro-2-nitronaphthalen-1-ol (Aldrich, U.S.A.), and 5,6,7,8-tetrahydro-1-nitronaphthalen-2-ol (Aldrich, U.S.A.).

**Reduction Reaction of Substituted Nitrophenols. General Procedure.** A solution of sodium borohydride (2.2 mmol) in 2 M NaOH (20 mL) added with 10% carbon−5% palladium was stirred at 0 °C under argon for 20 min. Next, the yellow solution of substituted nitrophenol (1 mol) in 2 M NaOH (5 mL) was added dropwise to the reagent mixture, which was stirred at 0 °C until the yellow color disappeared. The mixture (monitored by TLC) was then allowed to attain room temperature, quenched with 2 N HCl at 0°C, buffered with sodium acetate, and extracted with diethyl ether (3 × 25 mL). The ether layer was washed with brine and dried over anhydrous $Na_2SO_4$. The solvent was evaporated, and the crude product was used without further purification**.**

**Substituted 5*H*-Pyrido[3,2-*a*]phenoxazin-5-ones (1−12).** Substituted 2-aminophenols (0.01 mol) in methanol-acetic acid (50:50; vv, 10 mL) were added dropwise to an equimolar mixture of 5.8-quinolinquinone (0.01 mol) and Co(II) acetate (0.01 mol) in acetic acid (50 mL), stirred, and gently warmed until the dark color showed the complex formation. The reaction mixture refluxed for 2 h, was evaporated in vacuo, and acidified (6 N HCl) to break the Co complex, and extracted by chloroform. The organic layer, evaporated in vacuo and purified on silica gel column afforded pyridophenoxazinones **1**−**12** as main products, which were crystallized (EtOAc).

**5*H*-Benzo[*a*]pyrido[2,3-*j*]phenoxazin-5-one (10).** Mp 274−5 °C; UV ($CHCl_3$) $\lambda_{max}$ (log $\epsilon$) nm: 377.3 (3.04), 488.9 (3.11);$^1$H NMR ($CDCl_3$) 9.15 (1H, dd; $J$ = 4.3, 2,1 Hz), 8.71 (1H, dd; $J$ = 8.2, 2.1 Hz), 8.21 (1H, dd; $J$ = 7.8, 2.0 Hz), 7.88 (1H, d; $J$ = 7.8, 2.0 Hz), 7.70 (1H, dd; $J$ = 8.2, 4.3 Hz), 7.67 (1H, dt; $J$ = 7.8, 2.0), 7.65 (1H, dt; $J$ = 7.8, 2.0), 7.62 (1H, d; $J$ = 8.2 Hz), 7.44 (1H, d; $J$ = 8.2 Hz), 6.69 (1H, s), $^{13}$C NMR ($CDCl_3$) 182.23 (s), 155.10 (s), 154.58 (s), 153.60 (d), 147.62 (s), 145.20 (s), 142.29 (s), 135.81 (s), 134.81 (d), 131.30 (s), 131.22 (s), 129.05 (d), 128.33 (d), 127.21 (d), 126.15 (d), 123.82 (d), 115.07 (d), 111.21 (d), 106.05 (d); MS-EI *m*/*z* 298 (M+). Yield 16%. Anal. ($C_{19}H_{10}N_2O_2$) C, H, N.

**5*H*-Benzo[*i*]pyrido[3,2-*a*]phenoxazin-5-one (11).** Mp 279−5 °C; UV ($CHCl_3$) $\lambda_{max}$ (log $\epsilon$) nm: 375.2 (3.00), 411.9 (3.07); $^1$H NMR ($CDCl_3$) 9.11 (1H, dd; $J$ = 4.3, 1.8 Hz), 9.09 (1H, dd; $J$ = 7.5, 1.8 Hz), 8.37 (1H, s), 8.02 (1H, dd; $J$ = 7.8, 2.1 Hz), 7.89 (1H, dd; $J$ = 7.8, 2.1 Hz), 7.87 (1H, dt; $J$ = 7.8, 2.1 Hz), 7.75 (1H, dd; $J$ = 7.5, 4.3 Hz), 7.70 (1H, s), 7.62 (1H, dt; $J$ = 7.8, 2.1 Hz), 6.67 (1H, s);$^{13}$C NMR ($CDCl_3$) 182.30 (s), 153.52 (d), 152.81 (s), 174.22 (s), 146.31 (s), 144.15 (s), 139.70 (s), 133.71 (s), 133.33 (d), 131.31 (s), 131.15 (s), 129.20 (d), 127.45 (d), 125.76 (d), 125.53 (d), 125.27(d), 112.36 (d), 109.81 (d), 106.78 (s); MS-EI *m*/*z* 298 (M+). Yield 20%. Anal. ($C_{19}H_{10}N_2O_2$) C, H, N.

**5*H*-Benzo[*h*]pyrido[3,2-*a*]phenoxazin-5-one (12).** Mp 280−5 °C; UV ($CHCl_3$) $\lambda_{max}$ (log $\epsilon$) nm: 375.2 (3.19), 491.0 (3.17); $^1$H NMR ($CDCl_3$) 9.20 (1H, dd; $J$ = 2,1, 4.4 Hz), 9.69 (1H, dd; $J$ = 8.1, 2,0 Hz), 8.50 (1H, dd; $J$ = 6.4, 3.2 Hz), 8.11 (1H, d; $J$ = 8.4, Hz) 7.91 (1H, dd; $J$ = 6.4, 3.2 Hz), 7.81 (1H, d; $J$ = 8.4 Hz), 7.73 (1H, dd; $J$ = 8.0, 4.4 Hz), 7.70 (1H, dd; $J$ = 6.4, 3.2 Hz), 7.68 (1H, dd; $J$ = 6.4, 3.2 Hz), 6.70 (1H, s); $^{13}$C NMR ($CDCl_3$) 182.36 (s), 153.83 (d), 152.86 (s), 147.49 (s), 146.51 (s), 140.84 (s), 135.72 (s), 134.67 (d), 129,90 (s), 129.68 (d), 129.23 (s), 128.42 (d), 127.85 (s), 127.67 (d), 127.09 (d), 126.67 (d), 125.92 (d), 122.50 (d), 106.71 (s); MS-EI *m*/*z* 298 (M+). Yield 15%. Anal. ($C_{19}H_{10}N_2O_2$) C, H, N.

**Molecular Modeling.** Molecular modeling and graphical manipulations were performed using the SYBYL software package,[18] running on a Silicon Graphics R12000 workstation. The previously described model of PPH bound to the $[d(GAAGCTTC)]_2$ octamer[9] was used as a template to build the molecular models of the **10**/$[d(GAAGCTTC)]_2$, **11**/$[d(GAAGCTTC)]_2$, and **12**/$[d(GAAGCTTC)]_2$ complexes. All of the atoms were then fixed according to SYBYL atom types. Hydrogens were added and minimized using the MMFF94s force field and MMFF94 charges. The structures of the pyridophenoxazinones **10**−**12**, constructed in SYBYL and energy minimized with the Tripos force field[19] and Gasteiger-Hückel charges, were overlapped with the structure of PPH about the common quinolinquinonic moiety, and the structure of PPH was then removed. The resulting complexes were subsequently subjected to energy minimization using the MMFF94s force field with MMFF94 charges. During energy minimization, the structure of the pyridophenoxazinones was allowed to move, while the structure of the nucleic acid was frozen. The energy minimization was carried out performing 300 cycles of steepest descent energy minimization followed by conjugate gradient energy minimization until the energy difference was less than 0.05 kcal/mol Å.

**Biology. Compounds.** Test compounds were dissolved in DMSO at an initial concentration of 200 $\mu$M and then were serially diluted in culture medium.

**Cells.** Cell lines were from American Type Culture Collection (ATCC). Leukemia- and lymphoma-derived cells were grown in RPMI 1640 containing 10% fetal calf serum (FCS), 100 U/mL of penicillin G, and 100 $\mu$g/mL of streptomycin. Solid-tumor derived cells were grown in their specific media supplemented with 10% FCS and antibiotics. Cell cultures were incubated at 37 °C in a humidified 5% $CO_2$ atmosphere. Cell cultures were checked periodically for the absence of mycoplasma contamination by the Hoechst staining method.

**Antiproliferative Essays.** Exponentially growing leukemia and lymphoma cells were resuspended at a density of 1 × $10^5$ cells/mL in RPMI containing serial dilutions of the test drugs. Cell viability was determined after 96 h at 37 °C by the 3-(4,5-dimethylthiazol-2-yl)-2,5-diphenyl-tetrazolium bromide (MTT) method. Activity against solid-tumor derived cells was evaluated in exponentially growing cultures seeded at 5 × $10^4$ cells/mL and allowed to adhere for 16 h to culture plates before the addition of drugs. Cell viability was determined by the MTT method 4 days later.

**Linear Regression Analysis.** Tumor cell growth at each drug concentration was expressed as a percentage of untreated controls, and the concentration resulting in 50% ($IC_{50}$) growth inhibition was determined by linear regression analysis.

**DNA Unwinding Assays.** Negatively supercoiled pBR322 DNA was prepared using the Plasmid mega Kit (Qiagen, Valencia, CA) as described by the manufacturer. The relaxed pBR322 plasmid DNA used in unwinding assays was generated by treating negatively supercoiled pBR322 with calf thymus topoisomerase I (TopoGen, Inc.) relaxation buffer (10 mM Tris-HCl (pH 7.5), 175 mM KCl, 5 mM $MgCl_2$, 0.1 mM EDTA, and 2.5% glycerol) before the addition of other reaction components. Assay mixtures contained 5 nM relaxed pBR322 plasmid DNA, topoisomerase I (4.5 units), and the drug in 20 $\mu$L of relaxation buffer. The drugs employed in this study were **10** (1−50 $\mu$M), 100 $\mu$M etoposide (Sigma, St. Louis, MO), ethidium bromide (10 $\mu$M), or a DMSO control (final DMSO concentration was adjusted to 1% in all samples). Reactions were incubated for 30 min at 37 °C and stopped by extracting with an equal volume of phenol−chloroform. Aqueous samples (20 $\mu$L) were removed from the reactions, and 3 $\mu$L of stop solution (0.77% SDS, 77 mM NaEDTA (pH 8.0)) followed by 2 $\mu$L of agarose gel loading buffer (30% sucrose, in 10 mM Tris-HCl (pH 7.9)) were added to each. The samples were subjected to electrophoresis in a 1% agarose gel in TBE buffer (100 mM Tris-borate, 2 mM EDTA). The DNA bands were stained with 1 $\mu$g/mL of ethidium bromide and photographed under UV.

**Cell Cycle Analysis.** Control and treated HT-29 human colon carcinoma cells were harvested by enzymatic treatment (trypsin/EDTA 0.2%), washed in PBS w/o $Ca^{2+}$ and $Mg^{2+}$, and fixed in 70% ethanol for 24 h at 4C°. After a washing in PBSw/o $Ca^{2+}$ and $Mg^{2+}$, HT-29 cells were stained in 2 mL of propidium iodide (PI) staining solution (25 $\mu$g/mL of PI, 1 mg/mL of RNAse in PBS w/o $Ca^{2+}$ and $Mg^{2+}$ at pH 7.4) for 60 min at room temperature in the dark. DNA-flow cytometry was performed in duplicate by a

FACScan flow cytometer (Becton Dickinson, San Jose, CA) coupled with a CICERO signals interface module (Cytomation, Fort Collins, CO). Cell-cycle analysis was performed by ModFit LT software (Verity Software House Inc., MA). FL2 area versus FL2 width gating was done to exclude doublets from the G2/M region. For each sample, 15 000 events were stored in the list mode file.

**Topoisomerase I- and II-Mediated DNA Cleavage Assays.** The assays were performed as reported in the literature.[21−23] Supercoiled pBR322 DNA (0.5 $\mu$g) was incubated with 4 units of human topoisomerase I or II (TopoGen, Inc.) at 37 °C for 30 min in a relaxation buffer (50 mM Tris at pH 7.8, 50 mM KCl, 10 mM $MgCl_2$, 1 mM dithiothreitol, 1 mM EDTA, and ATP) in the presence of varying concentrations of the drug under study. Reactions were terminated by adding sodium dodecyl sulfate to 0.25% and proteinase K to 250 $\mu$g/mL. DNA samples were then added to the electrophoresis dye mixture (3 mL) and electrophoresed in a 1% agarose gel containing ethidium bromide (1 mg/mL) at room temperature for 2 h at 120 V. The gels were washed and photographed under UV light.

**Acknowledgment.** We are grateful to Professor Paolo La Colla and his team (University of Cagliari) for the antiproliferative tests. We thank the Centro Interdipartimentale di Metodologie Chimico-Fisiche and the Centro Interdipartimentale di Analisi Strumentale dell'Università di Napoli "Federico II". This work was supported by a grant from Italian MIUR (PRIN 2004).

**Supporting Information Available:** Analytical data (UV, $^1$H NMR, $^{13}$C, MS, mp) of compounds **1**−**9** and elemental analysis results of compounds **1**−**12**. This material is available free of charge via the Internet at http://pubs.acs.org.

## References

(1) Begleiter, A. Clinical Applications of Quinone-Containing Alkylating Agents. *Front. Biosci.* **2000**, *5*, E153-E171.
(2) Di Marco, A.; Cassinelli, G.; Arcamone, F. The Discovery of Daunorubicin. *Cancer Treat. Rep.* **1981**, *65*, 3−8.
(3) Wakelin, L. P. G.; Waring, M. J. DNA Intercalating Agents. In *Comprehensive Medicinal Chemistry*; Sammes. P. G., Ed.; Pergamon Press: Oxford, U.K., 1990; Vol 2, pp 703−724. (b) Carter, S. K.; Crooke, S. T. In *Mitomycin C: Current Status and New Developments*; Academic Press: New York, 1979.
(4) Rao, K. V., Cullen, W. P. Streptonigrin, an Antitumor Substance, I. Isolation and Characterization. *Antibiot. Ann.* **1959**, 950−953.
(5) Zucchi, R.; Danesi, R. Cardiac Toxicity of Antineoplastic Anthracyclines. *Curr. Med. Chem.: Anti-Cancer Agents* **2003**, *3*, 151−171.
(6) Thomas, X.; Le, Q. H.; Fiere, D. Anthracycline-Related Toxicity Requiring Cardiac Transplantation in Long-Term Disease-Free Survivors with Acute Promyelocytic Leukemia. *Ann. Hematol.* **2002**, *81*, 504−507.
(7) Chabner, B. A.; Allegra, C. J.; Curt, G. A.; Calabresi, P.; Antineoplastic Agents. In *Goodman and* Gilman's The Pharmacological Basis of Therapeutics, 9th ed.; Hardman, J. G., Limbird, L. E., Molinoff, P. B., Ruddon, R. W., Gilman, A. G., Eds.; McGraw-Hill: New York, 1996; pp 1233−1287.
(8) Lown, J. W. *Anthracycline and Anthracenedione-based Anticancer Agents*, Elsevier: Amsterdam, The Netherlands, 1988.
(9) Bolognese, A.; Correale, G.; Manfra, M.; Lavecchia, A.; Mazzoni, O.; Novellino, E.; Barone, V.; La Colla, P.; Loddo, R.; Murgioni, C.; Pani, A.; Serra, I.; Setzu, G. Antitumor Agents. 1. Synthesis, Biological Evaluation and Molecular Modeling of 5*H*-Pyrido[3,2-*a*]-phenoxazin-5-one, a New Compound with Potent Antiproliferative Activity. *J. Med. Chem.* **2002**, *45*, 5205−5216.
(10) Bolognese, A.; Correale, G.; Manfra, M.; Lavecchia, A.; Mazzoni, O.; Novellino, E.; Barone, V.; La Colla, P.; Loddo, R. Antitumor Agents. 2. Synthesis, Structure−Activity Relationships and Biological Evaluation of Substituted 5*H*-Pyridophenoxazin-5-ones with Potent Antiproliferative Activity. *J.* Med. Chem. **2002**, *45*, 5217−5223.
(11) Matsumoto, S. S.; Sidford, M. H.; Holden, J. A.; Barrows, L. R.; Copp, B. R. Mechanism of Action Studies of Cytotoxic Marine Alkaloids: Ascididemin Exhibits Thiol-Dependent Oxidative DNA Cleavage. *Tetrahedron Lett.* **2000**, *41*, 1667−1670.
(12) Shaikh, I. A.; Johnson, F.; Grollman, A. P. Streptonigrin 1. Structure−Activity Relationships Among Simple Bicyclic Analogues. Rate Dependence of DNA Degradation on Quinone Reduction Potential. *J. Med. Chem.* **1986**, *29*, 1329−1340.
(13) Alberti, A.; Bolognese, A.; Guerra, M.; Lavecchia, A.; Macciantelli, D.; Marcaccio, M.; Novellino, E.; Paolucci, F. Antitumor Agents. 4. Characterization of Free Radicals Produced During Reduction of the Antitumor Drug 5*H*-Pyridophenoxazin-5-one (PPH). An EPR Study. *Biochemistry* **2003**, *42*, 11924−11931.
(14) Yamamura, S. Oxidation of Phenols. In *The Chemistry of Phenols*, *Part I*; Rappoport, Z., Ed.; Patai Series; John Wiley & Sons: London, 2003; p 1153.
(15) Waring, M. J. Drugs and DNA: Uncoiling of the DNA Double Helix as Evidence of Intercalation. *Humangenetik* **1970**, *9*, 234−236.
(16) Pommier, Y.; Covey, J. M.; Kerrigan, D.; Markovits, J.; Pham, R. DNA Unwinding and Inhibition of Mouse Leukemia L1210 DNA Topoisomerase I by Intercalators. *Nucleic Acids Res.* **1987**, *25*, 6713−6731.
(17) Takusagawa, F.; Takusagawa, K. T.; Carlson, R. G.; Weaver, R. F. Selectivity of F8-Actinomycin D for RNA:DNA Hybrids and its Antileukemia Activity. *Bioorg. Med. Chem.* **1997**, *5*, 1197−1207.
(18) *SYBYL Molecular Modelling System*, version 6.2; Tripos Inc.: St. Louis, MO.
(19) Vinter, J. G.; Davis, A.; Saunders: M. R. Strategic Approaches to Drug Design. 1. An Integrated Software Framework for Molecular Modelling. *J. Comput.-Aided Mol. Des.* **1987**, *1*, 31−55.
(20) Chow, K.-C.; Ross, W. E. Topoisomerase-Specific Drug Sensitivity in Relation in Cell Cycle Progression. *Mol. Cell. Biol.* **1987**, 3119−3123. (b) Sleiman, R. J.; Catchpoole, D. R.; Stewart, B. W. Drug-Induced Death of Leukaemic Cells after G2/M Arrest: Higher Order DNA Fragmentation as an Indicator of Mechanism. *Br. J. Cancer* **1998**, *77*, 40−50.
(21) Bailly, C. DNA Relaxation and Cleavage Assays to Study Topoisomerase I Inhibitors. *Methods Enzymol*. **2001**, *340*, 610−623.
(22) Dassonneville, L.; Bonjean, K.; De Pauw-Gillet, M. C.; Colson, P.; Houssier, C.; Quetin-Leclercq, J.; Angenot, L.; Bailly, C. Stimulation of Topoisomerase II-Mediated DNA Cleavage by Three DNA-Intercalating Plant Alkaloids. Cryptolepine, Matadine and Serpentine. *Biochemistry* **1999**, *38*, 7719−7726.
(23) Dassonneville, L.; Wattez, N.; Baldeyrou, B.; Mahieu, C.; Lansiaux, A.; Banaigs, B.; Bonnard, I.; Bailly, C. Inhibition of Topoisomerase II by the Marine Alkaloid Ascididemin and Induction of Apoptosis in Leukemia Cells. *Biochem. Pharmacol.* **2000**, *60*, 527−537.

JM050745L